Thermal Conductance of Pressed Copper Contacts at Liquid Helium Temperatures

L. J. Salerno* and P. Kittel*
NASA Ames Research Center, Moffett Field, California
and
A. L. Spivak†
Trans-Bay Electronics, Richmond, California

The thermal contact conductance of a 0.4-μm surface finish OFHC copper sample pair has been investigated from 1.6 to 4.2 K for a range of applied contact forces up to 670 N. Experimental data have been fitted to the relation $\dot{Q} = \int \alpha T^n \, dT$ by assuming that the thermal contact conductance is a simple power function of the sample temperature. It has been found that the conductance is proportional to T^2 and that conductance increases with an increase in applied contact force. These results confirm earlier work.

Nomenclature

dT = incremental temperature difference
k = effective thermal contact conductance
n = exponent
$\dot{Q}$ = applied heater power
$\dot{Q}_0$ = offset heater power
ΔT = temperature difference across boundary
T = given temperature
$T\ell$ = lower sample temperature
T_{min} = minimum temperature obtained in measurement sequence
T_{max} = maximum temperature obtained in measurement sequence
Tu = upper sample temperature
s = standard deviation
α = proportionality constant

Introduction

THE optimum design of cryogenic instruments requires accurate thermal models. This is especially important for instruments where performance is sensitive to temperature. Infrared instruments such as the infrared astronomical satellite (IRAS) and the Space Infrared Telescope Facility (SIRTF) fall into this category. The present models are limited by a lack of knowledge of the low-temperature thermal conductance of the bolted joints that are typically used in the instrument-to-system interface. Previous studies of pressed contacts though limited in scope have shown that the thermal conductance does not obey the Wiedemann-Franz law (that states that the ratio of thermal to electrical conductivities is proportional to the temperature). In this paper, an effort to characterize the thermal conductance of pressed contacts at liquid helium-4 temperatures is described. Specifically, the dependence of thermal contact conductance on applied force and temperature is discussed.

Presented as Paper 83-1436 at the AIAA 18th Thermophysics Conference, Montreal, Canada, June 1-3, 1983; submitted Oct. 17, 1983; revision submitted Feb. 1984. This paper is declared a work of the U.S. Government and therefore is in the public domain.

*Research Scientist, Space Technology Branch, Space Science Division.
†Research Technician, NASA Ames Support Operations.

Theory and Previous Work

The phenomenon of thermal contact resistance is attributable to several factors; most notably, it is the consequence of contact being made only at discrete locations, rather than over the entire surface area. Ideally, the contact area is represented by the interface area of the surfaces themselves; however, a close examination reveals that even in the smoothest surfaces, irregularities exist which may restrict the contact area to as few as three discrete spots, irrespective of the sample dimensions. This theory is supported by experimental findings that contact resistance is dependent on the force of contact rather than contact area.[1,2] As the contact force increases, the material deforms. Thus, the area of initial contact increases and new spots develop. The heat flow is constricted in the vicinity of the contact locations because of the narrowness of the effective areas of contact. This constriction is in large part responsible for the contact resistance.[3,4] Estimates of the constriction resistance have been made for various assumed contact geometries by modeling the contacts as individual elements.[5] By arranging the elements in groups of varying heights, the case of surface waviness can be accounted for as well.[3,5]

A relation involving contact pressure and material hardness exists for determining the ratio of the surface area to the actual area of contact. However, the equivalent radius of the contact spot must be known and, at the present, there is no theoretical method available for general determination since each sample must be considered on an individual basis.[4] The height of the contact gap is also significant and a method does exist for its estimation.[3]

Additionally, the presence of surface films or oxides contributes to the problem. This is especially significant in the case of materials such as aluminum, which form oxides immediately in the presence of air. In the case of oxides, the oxide layer must be penetrated to obtain a consistent measure of the thermal resistance.

Although there has been significant interest[3,5-10] in the problem of contact resistance, estimation of the resistance from proposed theoretical models is still not a simple task. Principles of variational calculus have been applied to the problem to determine upper and lower bounds; however, because of the nature of the problem, there are limitations in the models and no satisfactory agreement exists between models due to the incompatibility of their boundary conditions. This poses a problem in predicting the behavior of pressed contacts and, therefore, most usable data in the field

Table 1 Copper sample pair 0.4-μm surface finish 22 N applied force

Bath temperature, K	α, mW/K^{n+1}	n	Q_0, mW	s, α	s, n	s, Q_0	$T_{\min}$, K	$T_{\max}$, K
3.8								
Ascending	0.1630	1.911	6.663 E-2	7.309 E-3	1.902 E-3	1.208 E-3	3.781	6.014
Descending	0.1649	1.917	7.678 E-2	1.967 E-3	7.486 E-3	7.487 E-3	3.781	5.982
3.6								
Ascending	0.1552	1.928	7.144 E-2	1.534 E-3	6.290 E-3	1.107 E-3	3.576	5.968
Descending	0.1784	1.882	1.371 E-1	1.882 E-3	6.742 E-3	1.274 E-3	3.576	5.968
3.4								
Ascending	0.1516	1.946	8.329 E-2	1.312 E-3	5.607 E-3	1.052 E-3	3.376	5.891
Descending	0.1742	1.893	1.568 E-1	1.594 E-3	5.937 E-3	1.221 E-3	3.379	5.824
3.2								
Ascending	0.1504	1.948	8.911 E-2	1.127 E-3	4.927 E-3	9.936 E-4	3.178	5.843
Descending	0.1704	1.901	1.552 E-3	1.370 E-3	5.285 E-3	1.144 E-3	3.211	5.785
3.0								
Ascending	0.1434	1.971	8.545 E-2	9.528 E-4	4.430 E-3	9.361 E-4	2.987	5.810
Descending	0.1595	1.932	1.439 E-1	1.118 E-3	4.679 E-3	1.064 E-3	3.002	5.749
2.4								
Ascending	—	—	—	—	—	—	—	—
Descending	—	—	—	—	—	—	—	—
2.0								
Ascending	—	—	—	—	—	—	—	—
Descending	—	—	—	—	—	—	—	—
1.6								
Ascending	—	—	—	—	—	—	—	—
Descending	—	—	—	—	—	—	—	—

Table 2 Copper sample pair 0.4-μm surface finish 45 N applied force

Bath temperature, K	α, mW/K^{n+1}	n	Q_0, mW	s, α	s, n	s, Q_0	$T_{\min}$, K	$T_{\max}$, K
3.8								
Ascending	0.1722	1.903	7.044 E-2	2.073 E-3	7.573 E-3	1.243 E-3	3.780	5.952
Descending	0.1847	1.911	7.576 E-2	8.190 E-3	8.190 E-3	1.316 E-3	3.834	3.834
3.6								
Ascending	0.1632	1.925	7.686 E-2	1.671 E-3	6.554 E-3	1.144 E-3	3.576	5.898
Descending	0.1986	1.879	1.361 E-1	2.250 E-3	7.317 E-3	1.335 E-3	3.576	5.728
3.4								
Ascending	0.1631	1.930	1.019 E-1	1.463 E-3	5.835 E-3	1.109 E-3	3.375	5.819
Descending	0.2001	1.871	1.639 E-1	1.952 E-3	6.404 E-3	1.285 E-3	3.380	5.664
3.2								
Ascending	0.1581	1.948	1.083 E-1	1.241 E-3	5.183 E-3	1.052 E-3	3.182	5.768
Descending	0.1853	1.913	1.555 E-1	1.576 E-3	5.657 E-3	1.191 E-3	3.207	5.627
3.0								
Ascending	0.1541	1.959	1.113 E-1	1.058 E-3	4.603 E-3	9.970 E-4	3.001	5.580
Descending	0.1778	1.930	1.468 E-1	1.300 E-3	4.950 E-3	1.093 E-3	3.001	5.580
2.4								
Ascending	0.7464 E-1	1.889	−4.711 E-3	3.881 E-4	3.986 E-3	2.947 E-4	2.572	4.802
Descending	—	—	—	—	—	—	—	—
2.0								
Ascending	—	—	—	—	—	—	—	—
Descending	—	—	—	—	—	—	—	—
1.6								
Ascending	—	—	—	—	—	—	—	—
Descending	—	—	—	—	—	—	—	—

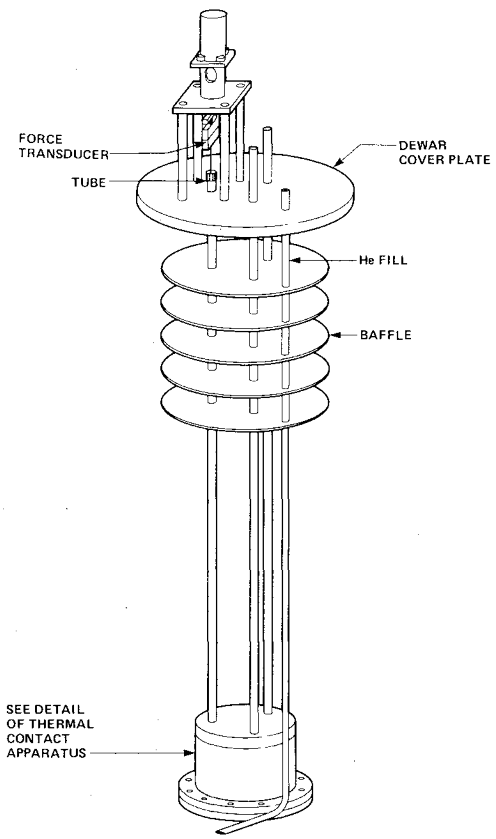

Fig. 1 Overall view of thermal contact apparatus.

are empirical. Additionally, an attempt to predict thermal conductance from the electrical conductance given by the Wiedemann-Franz relation yields values much less than those obtained empirically. It has been found that this discrepancy can be as large as a factor of 5×10^6 for contacts made at 4.2 K.[1]

Previous work consists of limited data for pressed contacts in the 4 K region.[1,2,11-14] Of these data, Cu-Cu results seem to dominate and, of the work surveyed, there seems to be good general agreement for the Cu-Cu conductance under applied forces of 450 N. Other work is limited to particular sample pairs and configurations, often corresponding to specific applications.[9,15] A need exists for more general thermal conductance data covering a variety of samples over a range of temperatures, contact forces, and surface conditions.

Experimental Procedure

An apparatus has been fabricated and tested which has been used to measure the thermal conductance of pressed sample pairs at temperatures from 1.6 to 4.2 K under applied forces of up to 700 N. The apparatus is pictured in Figs. 1 and 2. In operation, it is immersed in a Dewar filled with liquid helium 4. To obtain data below 4.2 K, the temperature of the liquid helium 4 is reduced by evaporative cooling. A pressure controller limits evacuation to achieve the desired temperature.

The following relation describes the mechanism of heat flow across the boundary between pressed solid surfaces:

$$\dot{Q}=k\Delta T \tag{1}$$

where $\dot{Q}$ is the thermal energy transferred across the boundary, k the effective thermal conductance of the contact, and ΔT the temperature difference across the boundary. While Eq. (1) is valid at any particular temperature T, k is actually a function of T so that

$$\dot{Q}=\int k(T)\,\mathrm{d}T \tag{2}$$

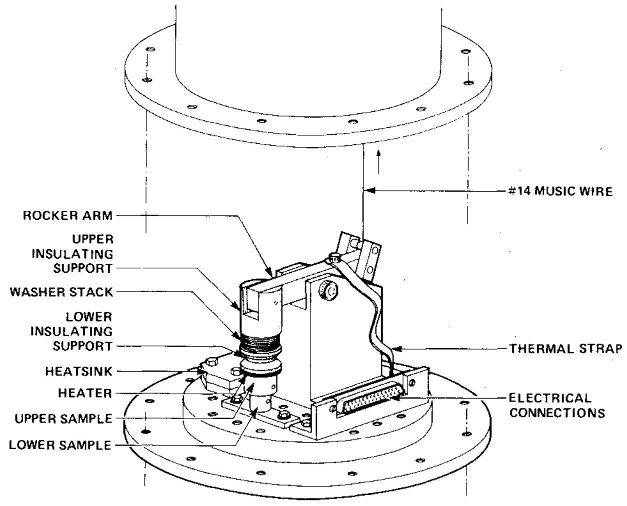

Fig. 2 Detail of cold plate.

If a simple power law is assumed to represent $k(T)$ and temperatures Tu and $T\ell$ as measured at each side of the boundary, it follows that

$$\dot{Q}=\int_{T\ell}^{Tu}\alpha T^n\,\mathrm{d}T=\frac{\alpha(Tu^{n+1}-T\ell^{\,n+1})}{n+1} \tag{3}$$

As discussed subsequently α and n are determined empirically for each sample pair, using Eq. (3).

The actual pressed contact sample pairs were fabricated from OFHC copper. The samples were cleaned and stored in a nitrogen environment to prevent contamination while not under test. Five pairs were prepared to evaluate the effect of different surface finishes on thermal conductance. Lapped surface finishes of 0.1, 0.2, 0.4, 0.8, and 1.6 μm rms were selected. Finishes were verified using a surface profilometer. All finishes were nominally flat. Each sample pair had the following dimensions: 10.2 mm diameter and 10.2 mm length for the lower sample, and 12.7 mm diameter and 8.89 mm length for the upper sample. The large diameter of the upper sample is to assure that any slight lateral movement would not prevent complete surface contact with the lower sample. A germanium resistance thermometer of 2.36 mm diameter and 6.1 mm length was installed in each sample. The axis of the thermometer was parallel to and located 2.36 mm from the interface. A heater consisting of manganin wire wound on an aluminum form was placed above the upper sample (see Fig. 2). An analysis was performed to determine the losses of heater power due to radiation and gas conduction. This analysis showed such losses to be negligible, assuring that the measured heater power was the power actually applied. Each sample pair was tested from 1.6 to 4.2 K over the range from 0 to 670 N. For each temperature and force value, heater powers from 0.100 mW to 10.0 mW were applied, the upper and lower sample temperatures measured after stabilization. Settling time was dependent on the charge of thermal flux. The criterion for stability was a minimum rate of change of temperature as obtained by measuring voltage of the germanium resistance thermometers. Typical settling times ranged from 45 s to 2.5 min. The force was then automatically incremented to the next value. In this manner, data sets were obtained for both ascending and descending values of the applied force, to assist in determining the magnitude of a hysteresis effect (if any). It should be noted that the apparatus was in all cases cooled down from room temperature with essentially zero applied force. Loading of the sample was performed during data acquisition only, and the load was relaxed when changing bath temperatures.

Results

Tables 1-8 present results obtained for the 0.4-μm surface finish Cu-Cu sample pair. The first column in the tables denotes the bath temperature at which the data were taken. (Tables 1-7 list results for both ascending and descending force values, while Table 8 gives the ascending value only, since 670 N is the upper force limit.) The next two columns give the derived values of α and n. These values were obtained from a computer program which fit the experimental values of heater power $\dot{Q}$, upper sample temperature Tu, and lower sample temperature $T\ell$ to Eq. (3). Since the conductance through the copper is much greater than the conductance of the contact, the bulk material contribution has been neglected and the ΔT obtained is simply the temperature difference between the upper and lower samples. The program also computes the magnitude of the offset in heater power Q_0 such that with no heater power applied a line fit of $\dot{Q}$ vs ΔT passes through the origin. The values of Q_0 are shown in column 3. In addition, the program performs a statistical analysis of the data in terms of the known uncertainties in the experimental measurements to calculate an uncertainty in the computed quantities α, n, and $\dot{Q}_0$. The next three columns give the standard deviation in the computed quantities α, n, and Q_0 as a measure of this error. The last two columns represent the minimum and maximum temperatures over which the computed values are accurate, representing the temperature range over which the original data were taken.

In addition to the values of α, n, and $\dot{Q}_0$, Tables 1-8 provide the respective error associated with these values. By specifying the uncertainty in the experimental data due to measurement accuracy and round-off errors, and perturbing these data assuming a Gaussian distribution, a standard deviation of the values' input to the computer program is obtained. Employing a random number generator, 99 computations of α, n and $\dot{Q}_0$ were performed by the program within the standard deviation in the output values of α, n, and $\dot{Q}_0$. In Fig. 3 the effective thermal conductance is plotted as a function of temperature for a range of applied forces. The curves shown in Fig. 3 were generated by averaging the values of α and n for both ascending and descending values of a particular force and plotting αT^n as a function of temperature.

Discussion

The values of the exponent n given in Tables 1-8 correspond well with earlier work. Berman[1] observed a nearly T^2 temperature dependence of thermal conductance at liquid helium temperatures. The present range of values $n=1.9$ to 2.2 certainly supports this finding.

Comparing the results in Fig. 3 with those of Berman[1] shows that, in particular, at an applied force of 670 N (150 lb), the value of 8.0×10^{-3} W/K is within a factor of 2 of Berman's value 1.46×10^{-2} W/K. Since Berman simply specifies a machine finish, it is felt that satisfactory agreement exists. Also shown is the effect of increasing applied force on thermal conductance. It is evident that the thermal conductance very definitely increases with increasing force, again supporting the earlier work of Berman.[1]

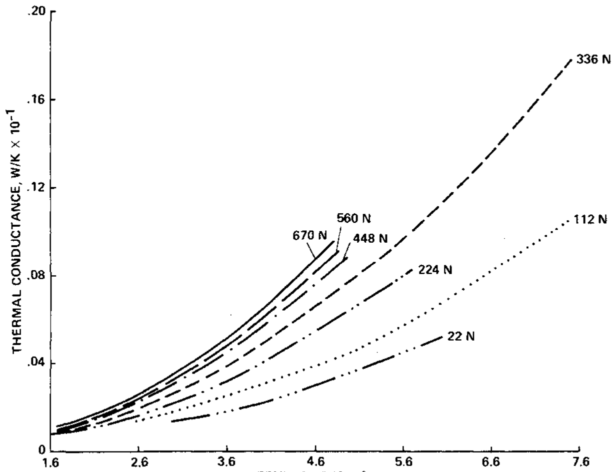

Fig. 3 Results for 0.4-μm copper sample pair.

Table 3 Copper sample pair 0.4-μm surface finish 112 N applied force

Bath temperature, K	α, mW/K^{n+1}	n	Q_0, mW	s, α	s, n	s, Q_0	T_{min}, K	T_{max}, K
3.8								
Ascending	0.2107	1.920	6.521 E-2	3.085 E-3	9.402 E-3	1.410 E-3	3.781	5.635
Descending	0.2531	1.891	7.155 E-2	1.076 E-2	4.193 E-3	1.567 E-3	3.780	5.464
3.6								
Ascending	0.2043	1.936	8.173 E-2	2.504 E-3	8.021 E-3	1.308 E-3	3.576	7.477
Descending	0.2463	1.920	1.261 E-1	3.523 E-3	9.487 E-3	1.545 E-3	3.576	5.353
3.4								
Ascending	0.2026	1.946	1.162 E-1	2.132 E-3	7.023 E-3	1.265 E-3	3.377	5.471
Descending	0.2459	1.921	1.614 E-1	2.961 E-3	8.142 E-3	1.473 E-3	3.381	5.273
3.2								
Ascending	0.2013	1.947	1.273 E-1	1.809 E-3	6.095 E-3	1.191 E-3	3.185	5.416
Descending	—	—	—	—	—	—	—	—
3.0								
Ascending	0.1964	1.957	1.281 E-1	1.5279 E-3	5.368 E-3	1.116 E-3	2.989	5.364
Descending	0.2246	1.969	1.447 E-1	1.9244 E-3	6.011 E-3	1.214 E-3	2.999	5.160
2.4								
Ascending	0.1135	2.029	−4.531 E-2	5.407 E-4	3.254 E-3	6.246 E-4	2.574	5.923
Descending	0.1479	2.060	−7.869 E-2	6.865 E-4	3.175 E-3	6.219 E-4	2.584	5.896
2.0								
Ascending	—	—	—	—	—	—	—	—
Descending	—	—	—	—	—	—	—	—
1.6								
Ascending	—	—	—	—	—	—	—	—
Descending	—	—	—	—	—	—	—	—

Table 4 Copper sample pair 0.4-μm surface finish 224 N applied force

Bath temperature, K	α, mW/K^{n+1}	n	Q_0, mW	s, α	s, n	s, Q_0	T_{min}, K	T_{max}, K
3.8								
Ascending	0.2745	1.967	5.847 E-2	5.626 E-3	1.352 E-2	1.777 E-3	3.780	5.239
Descending	0.3031	0.974	5.526 E-2	7.004 E-3	1.537 E-2	1.926 E-3	3.781	5.126
3.6								
Ascending	0.2653	1.990	7.878 E-2	4.4219 E-3	1.124 E-2	1.619 E-3	3.575	5.138
Descending	0.3050	1.981	1.155 E-1	5.848 E-3	1.305 E-2	1.862 E-3	3.576	5.008
3.4								
Ascending	0.2696	1.984	1.268 E-1	3.749 E-3	9.588 E-3	1.557 E-3	3.375	5.043
Descending	0.3115	1.971	1.595 E-1	4.899 E-3	1.095 E-2	1.764 E-3	3.379	4.912
3.2								
Ascending	0.2608	2.008	1.368 E-1	3.022 E-3	8.146 E-3	1.435 E-3	3.187	4.971
Descending	—	—	—	—	—	—	—	—
3.0								
Ascending	0.2532	2.022	1.318 E-1	2.430 E-3	6.891 E-3	1.294 E-3	2.991	4.906
Descending	0.2801	2.034	1.413 E-1	2.934 E-3	7.611 E-3	1.395 E-3	2.999	4.773
2.4								
Ascending	0.1564	2.049	−1.084 E-1	8.174 E-4	3.773 E-3	5.936 E-4	2.574	5.331
Descending	0.2167	2.073	−1.438 E-1	1.090 E-3	3.672 E-3	5.636 E-4	2.581	5.245
2.0								
Ascending	0.1550	2.079	−3.477 E-2	5.747 E-4	2.653 E-3	6.851 E-4	1.996	5.685
Descending	0.1965	2.120	−6.473 E-2	7.400 E-4	2.845 E-3	6.465 E-4	1.998	5.200
1.6								
Ascending	0.1591	2.122	−1.9940 E-2	5.420 E-4	2.509 E-3	7.372 E-4	1.687	5.506
Descending	0.1972	2.126	−3.4153 E-2	6.592 E-4	2.576 E-3	7.043 E-4	1.689	5.149

Table 5 Copper sample pair 0.4-μm surface finish 336 N applied force

Bath temperature, K	α, mW/K^{n+1}	n	Q_0, mW	s, α	s, n	s, Q_0	T_{min}, K	T_{max}, K
3.8								
Ascending	0.3173	2.008	4.811 E-2	8.180 E-3	1.726 E-2	2.054 E-3	3.783	5.033
Descending	0.3135	2.065	4.388 E-2	8.794 E-3	1.888 E-2	2.150 E-3	3.781	4.966
3.6								
Ascending	0.3177	1.008	7.727 E-2	6.593 E-3	1.423 E-2	1.880 E-3	3.576	7.479
Descending	—	—	—	—	—	—	—	—
3.4								
Ascending	0.3174	1.016	1.328 E-1	5.362 E-3	1.185 E-2	1.796 E-3	3.377	4.821
Descending	0.3388	2.026	1.524 E-1	6.265 E-3	1.306 E-2	1.952 E-3	3.380	4.745
3.2								
Ascending	0.3077	2.038	1.409 E-1	4.281 E-3	9.973 E-3	1.640 E-3	3.192	4.743
Descending	0.3287	2.045	1.532 E-1	4.946 E-3	1.082 E-2	1.761 E-3	3.207	4.676
3.0								
Ascending	0.3052	2.039	1.3811E-1	3.394 E-3	8.163 E-3	1.451 E-3	2.994	4.669
Descending	0.3114	2.079	1.389 E-1	3.711 E-3	8.809 E-3	1.522 E-3	2.998	4.590
2.4								
Ascending	0.1860	2.078	−1.219 E-1	1.009 E-3	4.050 E-3	5.841 E-4	2.574	5.019
Descending	0.2566	2.098	−1.791 E-1	1.292 E-3	3.814 E-3	5.348 E-4	2.481	4.941
2.0								
Ascending	0.2009	2.107	−6.573 E-2	7.539 E-4	2.839 E-3	6.444 E-4	2.000	5.195
Descending	0.2419	2.135	−9.460 E-2	9.243 E-4	3.014 E-3	6.069 E-4	1.998	4.860
1.6								
Ascending	0.2082	2.140	−4.602 E-2	6.983 E-4	2.623 E-3	6.921 E-4	1.686	5.033
Descending	0.2397	2.154	−6.216 E-2	7.971 E-4	2.687 E-3	6.630 E-4	1.689	4.800

Table 6 Copper sample pair 0.4-μm surface finish 448 N applied force

Bath temperature, K	α, mW/K^{n+1}	n	Q_0, mW	s, α	s, n	s, Q_0	T_{min}, K	T_{max}, K
3.8								
Ascending	0.3581	2.008	4.423 E-2	1.069 E-2	2.015 E-2	2.258 E-3	3.780	4.924
Descending	0.3679	2.021	4.063 E-2	1.159 E-2	2.134 E-2	2.329 E-3	3.780	4.885
3.6								
Ascending	0.3402	2.04822	6.919 E-2	8.081 E-3	1.645 E-2	2.042 E-3	3.575	4.805
Descending	—	—	—	—	—	—	—	—
3.4								
Ascending	0.3434	2.049	1.348 E-1	6.641 E-3	1.372 E-2	1.966 E-3	3.377	4.697
Descending	0.3686	2.030	1.511 E-1	7.507 E-3	1.449 E-2	2.077 E-3	3.379	4.658
3.2								
Ascending	.3411	2.053	1.449 E-1	5.333 E-3	1.132 E-2	1.792 E-3	3.201	4.586
Descending	—	—	—	—	—	—	—	—
3.0								
Ascending	0.3347	2.062	1.368 E-1	4.135 E-3	9.182 E-3	1.560 E-3	2.995	4.537
Descending	0.3441	2.072	1.402 E-1	4.4110 E-3	9.562 E-3	1.607 E-3	2.998	4.497
2.4								
Ascending	—	—	—	—	—	—	—	—
Descending	0.2868	2.096	−2.0011 E-1	1.434 E-3	3.879 E-3	5.146 E-4	2.436	4.778
2.0								
Ascending	0.2435	2.109	−8.929 E-2	9.211 E-4	2.974 E-3	6.066 E-4	1.995	4.898
Descending	0.2712	2.140	−1.143 E-1	1.045 E-4	3.111 E-3	5.844 E-4	1.995	4.691
1.6								
Ascending	0.2473	2.149	−6.712 E-2	8.206 E-4	2.697 E-3	6.559 E-4	1.688	4.763
Descending	0.2714	2.1520	−7.829 E-2	8.962 E-4	2.740 E-3	6.365 E-4	1.689	4.628

Table 7 Copper sample pair 0.4-μm surface finish 560 N applied force

Bath temperature, K	α, mW/K^{n+1}	n	Q_0, mW	s, α	s, n	s, Q_0	T_{min}, K	T_{max}, K
3.8								
Ascending	0.3892	2.004	4.183 E-2	1.273 E-2	2.221 E-2	2.397 E-3	3.780	4.858
Descending	0.3913	2.016	3.603 E-2	1.320 E-2	2.293 E-2	2.428 E-3	3.780	4.839
3.6								
Ascending	0.3758	2.032	8.104 E-2	9.743 E-3	1.804 E-2	2.198 E-3	3.577	4.739
Descending	0.3939	2.018	8.953 E-2	1.060 E-2	1.877 E-2	2.273 E-3	3.575	4.716
3.4								
Ascending	0.3756	2.0384	1.399 E-1	7.886 E-3	1.498 E-2	2.092 E-3	3.377	4.629
Descending	0.3760	2.0551	1.449 E-1	8.038 E-3	1.528 E-2	2.136 E-3	3.378	4.610
3.2								
Ascending	0.3608	2.066	1.447 E-1	5.998 E-3	1.211 E-2	1.876 E-3	3.199	4.532
Descending	0.3808	2.043	1.502 E-1	6.602 E-3	1.265 E-2	1.937 E-3	3.1	—
3.0								
Ascending	0.3529	2.079	1.388 E-1	4.668 E-3	9.904 E-3	1.641 E-3	2.997	4.462
Descending	0.3596	2.081	1.402 E-1	4.821 E-3	1.005 E-2	1.662 E-3	—	—
2.4								
Ascending	0.2798	2.063	−2.094 E-1	1.604 E-3	4.400 E-3	5.385 E-4	2.575	4.844
Descending	0.3029	2.104	−2.165 E-1	1.505 E-3	3.910 E-3	4.992 E-4	2.405	4.683
2.0								
Ascending	0.2749	2.123	−1.112 E-1	1.054 E-3	3.096 E-3	5.807 E-4	1.994	4.700
Descending	—	—	—	—	—	—	—	—
1.6								
Ascending	0.2776	2.153	−8.2519 E-2	—	—	—	—	—
Descending	0.2962	2.140	−8.808 E-2	9.700 E-4	2.767 E-3	6.184 E-4	1.689	4.528

Table 8 Copper sample pair 0.4-μm surface finish 672 N applied force

Bath temperature, K	α, mW/K^{n+1}	n	Q_0, mW	s, α	s, n	s, Q_0	T_{min}, K	T_{max}, K
3.8 Ascending	0.3989	2.017	3.616 E-2	1.382 E-2	2.359 E-2	2.469 E-3	3.780	4.822
3.6 Ascending	0.3809	2.054	8.068 E-2	1.046 E-2	1.918 E-2	2.276 E-3	3.577	4.699
3.4 Ascending	0.3928	2.037	1.450 E-1	8.623 E-3	1.571 E-2	2.169 E-3	3.377	4.591
3.2 Ascending	0.3829	2.053	1.496 E-1	6.674 E-3	1.274 E-3	1.946 E-4	3.196	4.514
3.0 Ascending	0.3677	2.078	1.400 E-1	5.034 E-3	1.029 E-2	1.685 E-3	2.997	4.423
2.4 Ascending	0.3058	2.118	−2.200 E-1	1.505 E-3	3.901 E-3	4.936 E-4	2.378	4.640
2.0 Ascending	—	—	—	—	—	—	—	—
1.6 Ascending	0.3013	2.151	−9.321 E-2	9.918 E-4	2.794 E-3	6.143 E-3	1.688	4.486

Conclusions

It has been shown that for the 0.4-μm OFHC copper pressed contact pair, the thermal conductance varies roughly as the second power of the temperature, and increases with increasing applied force.

Future work will focus on copper sample pairs of differing finishes as well as stainless steel, aluminum, and brass and silica glass samples. Also, the effect of such coatings as gold and indium on thermal contact conductance will be investigated.

Acknowledgments

The authors wish to acknowledge the contributions of C. Banda, G. Villere, and, especially, W. G. Marks, of Informatics, Inc., for their assistance in the area of software development.

References

[1] Berman, R., "Some Experiments on Thermal Contact at Low Temperatures," *Journal of Applied Physics,* Vol. 27, April 1956, pp. 318-323.

[2] Berman, R. and Mate, C. F., "Thermal Contact at Low Temperatures," *Nature*, Vol. 182, Dec. 13, 1958, pp. 1661-1663.

[3] Bobeth, M. and Diener, G., "Variational Bounds for the Effective Thermal Contact Resistance Between Bodies with Rough Surfaces," *International Journal of Heat and Mass Transfer*, Vol. 25, Jan. 1982, pp. 111-117.

[4] Jeng, D. R., "Thermal Contact Resistance in Vacuum," *Journal of Heat Transfer, Transactions of the ASME,* Vol. 89, Aug. 1967, pp. 275-276.

[5] Bobeth, M. and Diener, G., "Upper Bounds for the Effective Thermal Contact Resistance Between Bodies with Rough Surfaces," *International Journal of Heat and Mass Transfer,* Vol. 25, Aug. 1982, pp. 1231-1238.

[6] Cooper, M. G., Mikic, B. B., and Yovanovich, M. M., "Thermal Contact Conductance," *International Journal of Heat and Mass Transfer,* Vol. 12, March 1969, pp. 279-300.

[7] Mian, M. N., Al-Astrabadi, F. R., O'Callaghan, P. W., and Probert, S. D., "Thermal Resistance of Pressed Contacts Between Steel Surfaces: Influence of Oxide Films," *Journal of Mechanical Engineering Science*, Vol. 21, May 1979, pp. 159-166.

[8] Mikesell, R. P. and Scott, R. B., "Heat Conduction Through Insulating Supports in Very Low Temperature Equipment," *Journal of Research of National Bureau of Standards,* Vol. 57, Dec. 1956, pp. 371-378.

[9] Suomi, M., Anderson, A. C., and Holmstrom, B., "Heat Transfer Below 0.2 K," *Physica*, Vol. 38, March 1968, pp. 67-80.

[10] Thomas, T. R. and Probert, S. D., "Thermal Contact Resistance—The Directional Effect and Other Problems," *International Journal of Heat and Mass Transfer*, Vol. 13, May 1970, pp. 789-807.

[11] Deutsch, M., "Thermal Conductance in Screw-Fastened Joints at Helium Temperatures," *Cryogenics,* Vol. 18, May 1978, pp. 273-274.

[12] Manninen, M. and Zimmerman, W., "On the Use of Screw-Fastened Joints for Thermal Contact at Low Temperatures," *Review of Scientific Instruments,* Vol. 48, Dec. 1977, pp. 1710.

[13] Radebaugh, R., Siegwarth, J. D., Lawless, W. N., and Morrow, A. J., "Electrocaloric Refrigeration for Superconductors," National Bureau of Standards Rept. NBSIR 76-847, Feb. 1977, pp. 12 and 33.

[14] Wanner, M., "Thermal Conductance of a Pressed Al-Al Contact," *Cryogenics,* Vol. 21, Jan. 1981, pp. 4-6.

[15] Colwell, J. H., "The Performance of a Mechanical Heat Switch at Low Temperatures," *Review of Scientific Instruments,* Vol. 40, Sept. 1969, pp. 1182-1186.